

# Small signal analysis of memristor-based low-pass and high-pass filters using the perturbation theory

SUAYB CAGRI YENER<sup>a,\*</sup>, RESAT MUTLU<sup>b</sup>, H. HAKAN KUNTMAN<sup>c</sup>

<sup>a</sup>*Sakarya University, Electrical and Electronics Engineering Department, 54050, Sakarya, Turkey*

<sup>b</sup>*Namik Kemal University, Electronics and Communication Engineering Department, 59860, Corlu, Tekirdag, Turkey*

<sup>c</sup>*Istanbul Technical University, Electronics and Communication Engineering Department 34469, Istanbul, Turkey*

In this study, perturbation theory has been used for the first time in literature to do small-signal analysis and solution of the memristor-based low-pass and high-pass filters are given using perturbation theory. The time and frequency domain memristor-based filter behaviors are obtained analytically. It has been found that the second harmonic does exist and is dominant and its behavior as a function of frequency is inspected in these filters. The gain responses and the total harmonic distortions of the filters are also given. Results obtained from the perturbation theory are in good agreement with that of numerical simulations and this confirms the accuracy and the performance of the method.

(Received April 6, 2017; accepted February 12, 2018)

*Keywords:* Memristor, Analog applications, Memristor-based filters, Linear drift model, THD, Small-signal model, Perturbation theory

## 1. Introduction

Memristor had been claimed as a fundamental and nonlinear circuit element in 1971 and was declared to be found, almost four decades later, in 2008 [1, 2]. Memristor is a passive nonlinear circuit element and has interesting properties which cannot be mimicked by the other linear fundamental circuit elements such as resistor, inductor and capacitor [1]. It has a charge dependent resistance called memristance and has a zero-crossing pinched hysteresis loop when excited with an AC signal source. Due to these unusual properties, its feasibility for not only digital but also analog circuit applications are currently being investigated. There are already some studies on analog circuit applications of memristors in the [3–17] and some of them are about memristor-based analog filters [18–24].

Memristor is a nonlinear circuit element and therefore memristor-based low-pass (LP) and high-pass (HP) filters, made of a capacitor and a memristor connected in series, are also nonlinear circuits. Due to this nonlinearity, the equations describing memristor-capacitor (M-C) filters cannot be solved analytically. To the best of our knowledge, there is neither an exact nor an approximate analytical solution of the memristor-based LP and HP filters exist in the literature.

In this paper, using linear drift TiO<sub>2</sub> memristor model, small-signal analysis of both memristor-based low-pass and high-pass filters are done.

Since it is not possible to find exact solution of the differential equation describing the filter circuits, perturbation method, which is often used in quantum physics to find approximate solutions of the problems which cannot be solved exactly [25–28] is used for their small-signal analysis in steady-state for the first time in literature. Perturbation model simulation results are

compared to that of dynamic model simulations and it is shown that the perturbation model gives accurate results and able to predict current, voltage and hysteresis loops of the filters well. It is also shown that the harmonics do exist and the second harmonic is the dominant one. THD behavior of the memristor-based LP and HP filters are also examined in this study.

This paper is arranged as follows. In the second section, the linear dopant drift TiO<sub>2</sub> memristor model is given. In the third section, the memristor-based LP and HP filters are introduced and the dynamic models of the memristor-based low-pass and high-pass filters are presented. In the fourth section, the small signal analyses of both of the filters are done using the perturbation theory. In the fifth section, simulation results are given. Current, voltage, memristance and charge waveforms, hysteresis loops, gain and THD responses of the filters are obtained and compared by using simulations results of both small signal and dynamic models of the memristor-based filters. Paper is finished with conclusion.

## 2. TiO<sub>2</sub> linear drift modeling of memristor

A memristor is defined as either flux or charge controlled [1]. The instantaneous memristor charge is equal to the integration of its current with respect to time and given as

$$q(t) = \int_{-\infty}^t i(\tau) d\tau \quad (1)$$

The terminal equation of the charge-controlled memristor is given as

$$v(t) = M(q)i(t) \quad (2)$$

In this work, the charge dependent TiO<sub>2</sub> linear drift model of memristor given in [2] is used. Based on the linear dopant drift model, the memristor's charge-dependent resistance or memristance is given as

$$M(q) = \frac{d\varphi}{dq} = R_{OFF} \left( 1 - \frac{\mu_v R_{ON}}{D^2} q(t) \right) \quad (3)$$

Where  $D$  is the length of the memristive device,  $\mu$  is mobility of dopants,  $R_{ON}$  and  $R_{OFF}$  are low and high state resistances, respectively. For the simplicity we will use (4) defining memristance function in this study:

$$M(q) = M_0 - K_q q(t) \quad (4)$$

Where  $M_0 = R_{OFF}$  is the maximum memristance and  $K_q$  is the charge coefficient. Memristor charge can take values from 0 to  $q_{sat}$  for the memristor model given in [2]. Memristance is equal to  $M_0$  if the memristor is saturated at  $q=0$ . If the memristor is saturated at the maximum memristor charge,  $q=q_{sat}$ , its memristance becomes minimum and is equal to

$$M_{sat} = M_0 - K_q q_{sat} \quad (5)$$

If the memristor is not saturated;

$$M_0 > M(q) > M_{sat} \quad (6)$$

### 3. Dynamic models of memristor-based low pass and high pass filters

#### 3.1. The memristor-based low-pass and high-pass filters

Traditional R-C low-pass and high-pass filters are shown in

Fig. 1 (a) and (c), respectively. By replacing the linear resistor with a memristor, the memristor-based LP and HP filters are obtained as illustrated in

Fig. 1 (b) and (d) respectively. Both of the filters have adjustable gain and cut-off frequency characteristic due to the fact that memristor memristance can change as a function of memristor charge.

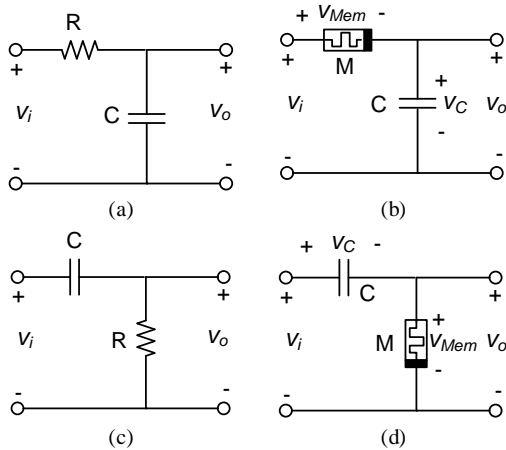


Fig. 1. (a), (c) RC low-pass and high-pass filters, respectively. (b), (d) memristor-based (MC) low-pass and high-pass filters, respectively

#### 3.2. Dynamic model of memristor based low pass and high pass filters

Memristance of a memristor is a nonlinear function. Assuming there is no saturation in the memristor-based LP and HP filters, their state-space representations are same and it is given as

$$\frac{dq_{Mem}}{dt} = i_{Mem} = \frac{v_i - v_C}{M(q)} = \frac{v_i - v_C}{M_0 - K_q q_{Mem}} \quad (7)$$

$$\frac{dv_C}{dt} = \frac{1}{C} i_C = \frac{i_{Mem}}{C} = \frac{v_i - v_C}{M(q)C} \quad (8)$$

Assuming the input voltage is sinusoidal, (7) and (8) can be combined as

$$v_i = V_m \sin(\omega t) = (M_0 - K_q q_{Mem}) i_{Mem} + v_C \quad (9)$$

The memristor current is also equal to the capacitor current:

$$i_{Mem} = \frac{dq_{Mem}}{dt} = \frac{dq_C}{dt} \quad (10)$$

By taking the integration of (10),

$$q_C(t) = q_{Mem}(t) + A \quad (11)$$

$A$  is the integration constant and equal to

$$A = q_C(0) - q_{Mem}(0) \quad (12)$$

Then, (9) turns into

$$V_m \sin(\omega t) = M(q) \frac{dq_{Mem}}{dt} + \frac{q_C}{C} \quad (13)$$

$$V_m \sin(\omega t) = M(q) \frac{dq_{Mem}}{dt} + \frac{q_{Mem} + A}{C} \quad (14)$$

### 4. Analysis of memristor based low-pass and high-pass filters based on the perturbation theory

#### 4.1. Small signal analysis of memristor based low pass and high pass filters with perturbation theory

(14) describes the behavior of both of the filters. An exact analytical solution for the memristor charge,  $q_{Mem}$ , in time or frequency domain cannot be obtained. Since (14) is not analytically solvable, the perturbation method is used to find an approximate solution for it.

The memristor charge is taken to be equal to

$$q_{Mem} = q = \bar{q} + \tilde{q} \quad (15)$$

Where  $\bar{q}$  is the average memristor charge and  $\tilde{q}$  is the memristor charge perturbation or the charge ripple. Then, the memristance is equal to

$$M(q) = M_0 - K_q q = M_0 - K_q \bar{q} - K_q \tilde{q} = \bar{M} - K_q \tilde{q} \quad (16)$$

where  $\bar{M}$  is the average memristance for one electrical period. Then, (9) turns into

$$\begin{aligned} v_{in}(t) &= (M_0 - K_q \bar{q} - K_q \tilde{q}) \frac{d\tilde{q}}{dt} + \frac{q + A}{C} \\ &= (\bar{M} - K_q \tilde{q}) \frac{d\tilde{q}}{dt} + \frac{\tilde{q}}{C} + \frac{\bar{q} + A}{C} \end{aligned} \quad (17)$$

$$v_m(t) = V_m \sin(\omega t) = \bar{M} \frac{d\tilde{q}}{dt} - K_q \tilde{q} \frac{d\tilde{q}}{dt} + \frac{\tilde{q}}{C} + \frac{\bar{q} + A}{C} \quad (18)$$

A small parameter is needed for being able to solve (18) using Perturbation method. The following arrangements are done for this purpose. By dividing each side of (18) by  $\bar{M}$ :

$$\frac{V_m \sin(\omega t)}{\bar{M}} = \frac{d\tilde{q}}{dt} + \frac{\tilde{q}}{\bar{M}C} - \frac{K_q}{\bar{M}} \tilde{q} \frac{d\tilde{q}}{dt} + \frac{\bar{q} + A}{\bar{M}C} \quad (19)$$

And by multiplying each side of (19) by  $C$ :

$$\frac{CV_m \sin(\omega t)}{\bar{M}} = C \frac{d\tilde{q}}{dt} + \frac{\tilde{q}}{\bar{M}} - \frac{K_q C}{\bar{M}} \tilde{q} \frac{d\tilde{q}}{dt} + \frac{\bar{q} + A}{\bar{M}} \quad (20)$$

$\varepsilon$  is assumed to be a small parameter and is equal to

$$\varepsilon = \frac{K_q C}{\bar{M}} \quad (21)$$

(20) can be rearranged as

$$\frac{CV_m \sin(\omega t)}{\bar{M}} = C \frac{d\tilde{q}}{dt} + \frac{\tilde{q}}{\bar{M}} - \varepsilon \tilde{q} \frac{d\tilde{q}}{dt} + \frac{\bar{q} + A}{\bar{M}} \quad (22)$$

Then, the solution of the memristor charge ripple can be assumed as

$$\begin{aligned} \tilde{q}(t) &= q_0(t) + \varepsilon q_1(t) + \varepsilon^2 q_2(t) \\ &\quad + \varepsilon^3 q_3(t) + \dots + \varepsilon^n q_n(t) \end{aligned} \quad (23)$$

Where  $q_0(t)$  is the zero<sup>th</sup> order solution,  $q_1(t)$  is the first order solution, and so on. If the zero<sup>th</sup> order solution,  $q_0(t)$ , is sought for, it is assumed that  $\varepsilon = 0$ . Then, (22) turns into

$$\frac{CV_m \sin(\omega t)}{\bar{M}} = C \frac{dq_0}{dt} + \frac{q_0}{\bar{M}} + \frac{\bar{q} + A}{\bar{M}} \quad (24)$$

The zero<sup>th</sup> order solution is

$$q_0(t) = Be^{-\frac{t}{\bar{M}C}} + \bar{q} + A + \frac{CV_m \sin(\omega t - \arctan(\omega \bar{M}C))}{\sqrt{1 + (\omega \bar{M}C)^2}} \quad (25)$$

Since we are interested in AC periodic steady-state solution, the homogenous solution part of (25) is not dealt with anymore. The average value of the input voltage is

$$\langle v(t) \rangle = \langle V_m \sin(\omega t) \rangle = \langle v_{Mem} \rangle + \langle v_C \rangle = 0 \quad (26)$$

This requires that these follows also must be true in steady state:

$$\langle v_C \rangle = \left\langle \frac{q_C}{C} \right\rangle = \left\langle \frac{\bar{q} + A}{C} \right\rangle = 0 \quad (27)$$

and

$$\langle v_{Mem} \rangle = \left\langle \frac{d\varphi}{dt} \right\rangle = 0. \quad (28)$$

Therefore, the average value of the memristor charge ripple is

$$\langle \tilde{q} \rangle = 0 \quad (29)$$

The average value of the capacitor charge is

$$\langle q_C \rangle = \langle \bar{q} + A \rangle = 0 \quad (30)$$

Therefore,  $A$  is equal to  $-\bar{q}$ . Also, when the transient

dies, in the periodic steady-state, the transient term,  $Be^{-\frac{t}{\bar{M}C}}$  must disappear. Then,

$$q_0(t) = \frac{CV_m \sin(\omega t - \arctan(\omega \bar{M}C))}{\sqrt{1 + (\omega \bar{M}C)^2}} \quad (31)$$

It is interesting to note that this is also same as the steady-state solution of an R-C series circuit whose resistance is equal to  $\bar{M}$ . If the first order solution,  $q_1(t)$ , is sought for, it should be assumed that  $\varepsilon$  is a small number not being equal to zero but its higher powers are negligible;  $\varepsilon^2 = \varepsilon^3 = \dots = \varepsilon^n = 0$  and the total solution of the memristor charge ripple is equal to the sum of the zero<sup>th</sup> solution and  $\varepsilon$  times the first order solution:

$$\tilde{q}(t) = q_0(t) + \varepsilon q_1(t) \quad (32)$$

And submitting (32) into (22):

$$\begin{aligned} \frac{CV_m \sin(\omega t)}{\bar{M}} &= C(q_0 + \varepsilon q_1)' + \frac{q_0 + \varepsilon q_1}{\bar{M}} \\ &\quad - \varepsilon(q_0 + \varepsilon q_1)(q_0 + \varepsilon q_1)' + \frac{\bar{q} + A}{\bar{M}} \end{aligned} \quad (33)$$

By rearranging (33):

$$\begin{aligned} \frac{CV_m \sin(\omega t)}{\bar{M}} - Cq_0' - \frac{q_0}{\bar{M}} - \frac{\bar{q} + A}{\bar{M}} \\ - \varepsilon \left( Cq_1' + \frac{q_1}{\bar{M}} - (q_0 q_0' + \varepsilon q_0 q_1' + \varepsilon q_0' q_1 + \varepsilon^2 q_1 q_1') \right) = 0 \end{aligned} \quad (34)$$

The left side of (35) is equal to zero and the following can also be seen from (35):

$$\varepsilon Cq_1' + \varepsilon \frac{q_1}{\bar{M}} - \varepsilon q_0 q_1' - \varepsilon^2 q_0 q_1' - \varepsilon^2 q_0' q_1 - \varepsilon^3 q_1 q_1' = 0 \quad (35)$$

By remembering that  $\varepsilon^2 = \varepsilon^3 = \dots = \varepsilon^n = 0$ , the differential equation is simplified to be

$$Cq_1' + \frac{q_1}{\bar{M}} - q_0 q_1' = 0 \quad (36)$$

$$\bar{M}Cq'_1 + q_1 = \bar{M}q_0q'_0 \quad (37)$$

Taking derivative of (31) by respect to time:

$$q'_0(t) = \frac{\omega CV_m}{\sqrt{1+(\omega\bar{M}C)^2}} \cos(\omega t - \arctan(\omega\bar{M}C)) \quad (38)$$

Then multiplying (31) by its derivative given in (38) and using the trigonometric identity,

$$\sin(2\phi) = 2\sin\phi\cos\phi \quad (39)$$

$$q_0q'_0 = \frac{C^2V_m^2\omega}{2(1+(\omega\bar{M}C)^2)} \sin(2\omega t - 2\arctan(\omega\bar{M}C)) \quad (40)$$

By submitting (40) into (37),

$$\begin{aligned} \bar{M}Cq'_1 + q_1 &= \frac{\bar{M}C^2V_m^2\omega}{2(1+(\omega\bar{M}C)^2)} \sin(2\omega t - 2\arctan(\omega\bar{M}C)) \end{aligned} \quad (41)$$

As  $q_0$  is found for (24), the solution of (41) in the periodic steady-state is similarly found as

$$\begin{aligned} q_1(t) &= \frac{\omega\bar{M}C^2V_m^2}{2(1+(\bar{M}C)^2)\sqrt{1+(2\omega\bar{M}C)^2}} \\ &\cdot \sin(2\omega t - 2\arctan(\omega\bar{M}C) - \arctan(2\omega\bar{M}C)) \end{aligned} \quad (42)$$

Then, the memristor charge ripple,  $\tilde{q}(t)$ , can be assumed to be equal to the sum of the zero<sup>th</sup> and the first order solutions:

$$\begin{aligned} \tilde{q}(t) = q_0 + \varepsilon q_1 &= \frac{CV_m \sin(\omega t - \arctan(\omega\bar{M}C))}{\sqrt{1+(\bar{M}C)^2}} + \left( \frac{K_q C}{\bar{M}} \right) \\ &\cdot \frac{\omega\bar{M}C^2V_m^2 \sin(2\omega t - 2\arctan(\omega\bar{M}C) - \arctan(2\omega\bar{M}C))}{2(1+(\omega\bar{M}C)^2)\sqrt{1+(2\omega\bar{M}C)^2}} \end{aligned} \quad (43)$$

By remembering (15),

$$\begin{aligned} q(t) &= \frac{CV_m \sin(\omega t - \arctan(\omega\bar{M}C))}{\sqrt{1+(\omega\bar{M}C)^2}} \\ &+ \frac{K_q C^3 V_m^2 \omega \sin(2\omega t - 2\arctan(\omega\bar{M}C) - \arctan(2\omega\bar{M}C))}{2(1+(\omega\bar{M}C)^2)\sqrt{1+(2\omega\bar{M}C)^2}} + \bar{q} \end{aligned} \quad (44)$$

The filter current or the memristor current is

$$\begin{aligned} i(t) = q'(t) &= \frac{\omega CV_m \cos(\omega t - \arctan(\omega\bar{M}C))}{\sqrt{1+(\omega\bar{M}C)^2}} \\ &+ \frac{\omega^2 K_q C^3 V_m^2 \cos(2\omega t - 2\arctan(\omega\bar{M}C) - \arctan(2\omega\bar{M}C))}{(1+(\omega\bar{M}C)^2)\sqrt{1+(2\omega\bar{M}C)^2}} \end{aligned} \quad (45)$$

The capacitor charge is

$$\begin{aligned} q_c(t) = q(t) - A &= \frac{CV_m \sin(\omega t - \arctan(\omega\bar{M}C))}{\sqrt{1+(\omega\bar{M}C)^2}} \\ &+ \frac{K_q C^3 V_m^2 \omega \sin(2\omega t - 2\arctan(\omega\bar{M}C) - \arctan(2\omega\bar{M}C))}{2(1+(\omega\bar{M}C)^2)\sqrt{1+(2\omega\bar{M}C)^2}} \end{aligned} \quad (46)$$

Then, the capacitor voltage is

$$\begin{aligned} v_c(t) = \frac{q_c(t)}{C} &= \frac{V_m \sin(\omega t - \arctan(\omega\bar{M}C))}{\sqrt{1+(\omega\bar{M}C)^2}} \\ &+ \frac{K_q C^2 V_m^2 \omega \sin(2\omega t - 2\arctan(\omega\bar{M}C) - \arctan(2\omega\bar{M}C))}{2(1+(\omega\bar{M}C)^2)\sqrt{1+(2\omega\bar{M}C)^2}} \end{aligned} \quad (47)$$

The memristor voltage can be found as

$$\begin{aligned} v_{Mem}(t) = v_i(t) - v_c(t) &= V_m \sin(\omega t) - v_c(t) \quad (48) \\ v_{Mem}(t) \cong V_m \sin(\omega t) &- \frac{V_m \sin(\omega t - \arctan(\omega\bar{M}C))}{\sqrt{1+(\omega\bar{M}C)^2}} \\ &- \frac{K_q C^2 V_m^2 \omega \sin(2\omega t - 2\arctan(\omega\bar{M}C) - \arctan(2\omega\bar{M}C))}{2(1+(\omega\bar{M}C)^2)\sqrt{1+(2\omega\bar{M}C)^2}} \end{aligned} \quad (49)$$

If the fundamental component is rearranged, (49) turns into

$$\begin{aligned} v_{Mem}(t) \cong &\frac{\omega C \bar{M} V_m \cos(\omega t - \arctan(\omega\bar{M}C))}{\sqrt{1+(\omega\bar{M}C)^2}} \\ &- \frac{K_q C^2 V_m^2 \omega \sin(2\omega t - 2\arctan(\omega\bar{M}C) - \arctan(2\omega\bar{M}C))}{2(1+(\omega\bar{M}C)^2)\sqrt{1+(2\omega\bar{M}C)^2}} \end{aligned} \quad (50)$$

## 4.2. Gain of the memristor-based low-pass and high-pass filters

In this section, the gain formulas for the memristor-based LP and HP filters are derived using the results of Section 4.1.

### 4.2.1. Gain of the memristor-based low-pass filter

The output voltage is the capacitor voltage for LP filter. As seen from (47), the output voltage has harmonics. Due to the harmonics, the gain of the of the LP filter is calculated from the fundamentals of the input and output signals and is equal to

$$G_{LPdB}(\omega) = 20 \log_{10} \left( \frac{(V_C)_{RMS}}{(V_{IN})_{RMS}} \right) = 20 \log_{10} \left( \frac{1}{\sqrt{1+(\omega C \bar{M})^2}} \right) \quad (51)$$

#### 4.2.2. Gain of the memristor-based high-pass filter

The output voltage is the memristor voltage for HP filter. Due to the harmonics, the gain of the of the HP filter is calculated from the fundamentals of the input and output signals and is equal to

$$G_{HPdB}(\omega) = 20 \log_{10} \left( \frac{(V_1)_{RMS}}{(V_m)_{RMS}} \right) = 20 \log_{10} \left( \frac{\omega C \bar{M}}{\sqrt{1 + (\omega C \bar{M})^2}} \right) \quad (52)$$

#### 4.3. Total harmonic distortion of the memristor-based low-pass and high-pass filters

In this section, the total harmonic distortion (THD) formulas for the memristor-based LP and HP filters are derived using the results of Section 0.

##### 4.3.1. THD of the memristor-based low-pass filter

The THD of the memristor-based LP filter is given as

$$THD_{LP}(\omega) = \frac{(V_2)_{RMS}}{(V_1)_{RMS}} = \frac{\omega K_q C^2 V_m}{2 \sqrt{1 + (\omega C \bar{M})^2} \sqrt{1 + (2\omega \bar{M} C)^2}} \quad (53)$$

The frequency at which, THD of the M-C LP filter becomes the maximum, can be calculated by taking the derivative of THD by respect to  $\omega$ :

$$\frac{\partial THD_{LP}}{\partial \omega} = \frac{K_q C^2 V_m}{2} \frac{\sqrt{1 + (\omega \bar{M} C)^2} (1 + (2\omega \bar{M} C)^2) - K_q C^2 V_m}{(1 + (\omega \bar{M} C)^2) (1 + (2\omega \bar{M} C)^2)} - \frac{K_q C^2 V_m}{2} \frac{\left( \frac{1}{2} \frac{2\omega (\bar{M} C)^2 \sqrt{1 + (2\omega \bar{M} C)^2}}{\sqrt{1 + (\omega \bar{M} C)^2}} + \frac{1}{2} \frac{8\omega (\bar{M} C)^2 \sqrt{1 + (\omega \bar{M} C)^2}}{\sqrt{1 + (2\omega \bar{M} C)^2}} \right)}{(1 + (\omega \bar{M} C)^2) (1 + (2\omega \bar{M} C)^2)} \quad (54)$$

= 0

The THD is found to be zero at  $\omega = 0$  and  $\omega = \infty$  rad/s. It is maximum at

$$\omega = \frac{1}{\sqrt{2} \bar{M} C} = \frac{\omega_c}{\sqrt{2}} \quad (55)$$

(55) shows an inherent property of all the linear dopant drift TiO<sub>2</sub> memristor model-based LP filters for small signals when the harmonics other than the second harmonic is negligible. The high frequency behavior of the memristor results in low distortion at high frequencies. Also the maximum distortion of the M-C LP filter is

$$(THD_{LP})_{MAX}(\omega) = \frac{\omega K_q C^2 V_m}{2 \sqrt{1 + (\omega C \bar{M})^2} \sqrt{1 + (2\omega \bar{M} C)^2}} = \frac{K_q C V_m}{6 \bar{M}} \quad (56)$$

As seen from (53) and (56), the total harmonic distortion of the Memristor-based LP Filter is zero at zero frequency, starts increasing with increasing frequency and it has a maximum point occurring at a frequency equal to

$1/\sqrt{2}$  times the cut-off frequency and, after this frequency, the distortion decreases with increasing frequency and disappears at very high frequencies since the memristor starts behaving as if a linear time invariant resistor.

The THD behavior of the memristor-based low-pass filter can be explained as that at low frequency the capacitive reactance of the filter is dominant and the memristor nonlinearity is suppressed, at high frequency the capacitive reactance is negligible and also the memristor behaves as a resistor, there is a frequency region in which filter THD is not negligible and has a maximum. For the operation frequencies near the maximum THD frequency, the signal amplitude should be kept low for a good performance.

##### 4.3.2. THD of the memristor-based high-pass filter

The THD of the memristor-based HP filter is given as

$$THD_{HP}(\omega) = \frac{(V_2)_{RMS}}{(V_1)_{RMS}} = \frac{K_q C V_m}{2 \bar{M} \sqrt{1 + (\omega C \bar{M})^2} \sqrt{1 + (2\omega \bar{M} C)^2}} \quad (57)$$

(57) is a monotonously decreasing function and the THD of the memristor-based HP filter becomes negligible at high frequencies. The maximum THD of the memristor-based HP filter occurs at zero frequency and is equal to

$$(THD_{HP})_{MAX}(\omega) = THD(\omega = 0) = \frac{K_q C V_m}{2 \bar{M}} \quad (58)$$

Also it can be seen that the maximum THD of the M-C HP filter is higher than that of the M-C LP filter:

$$(THD_{HP})_{MAX}(\omega) = 3 \times (THD_{LP})_{MAX}(\omega) \quad (59)$$

### 5. Simulations of memristor based low-pass and high-pass filters

In this section, simulations are done to compare the results of dynamic and small signal models. For M-C LP filter, the output voltage is the capacitor voltage,  $v_C$ , and for M-C HP filter, the output voltage is the memristor voltage,  $v_{Mem}$ . In this section, M-C LP and HP filters are simulated for several frequencies. A sinusoidal input voltage of  $v(t) = V_m \times \sin(\omega t)$  is applied to the filter. Unless otherwise stated all simulations are performed for  $V_m = 0.5V$ ,  $C = 200nF$ ,  $M_0 = 20k\Omega$ ,  $M_{SAT} = 100\Omega$ ,  $q_{SAT} = 1\mu C$ . In the general sense, reasonable filter parameters are chosen to make  $\varepsilon$  a small number for the simulations.

#### 5.1. Time domain simulations of memristor based low-pass and high-pass filters

LP and HP filter time domain waveforms are shown in Fig. 2 for  $f = 1Hz$  and  $f = 1kHz$ , respectively. The simulation results obtained by both of the models match

well as shown in Fig. 2 and Fig. 3. As shown in Fig. 2, the memristor behavior in the filter is obvious at  $f=1$  Hz: the memristor has a zero-crossing hysteresis loop, its memristance and charge vary by time, its current is not sinusoidal at the steady-state due to its nonlinearity. As shown in Fig. 3, at  $f=1$  kHz, the memristor starts behaving as a linear time invariant (LTI) resistor, its memristance and charge are almost constant, its hysteresis loop disappears, its current is almost sinusoidal, and the M-C filter behaves similar to a LTI R-C filter.

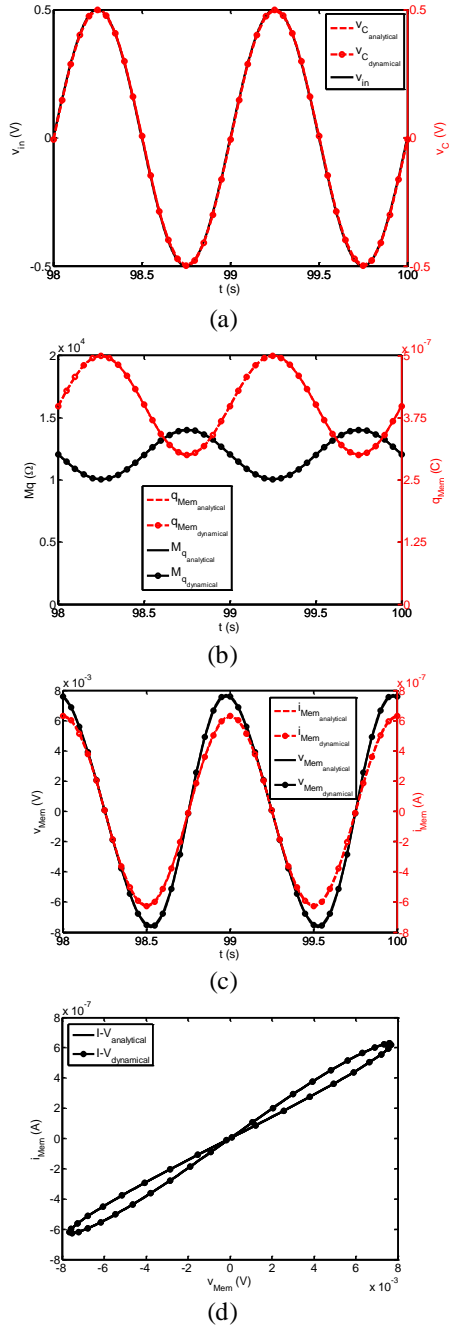


Fig. 2. M-C LP and HP filters time domain wave forms obtained using small signal and dynamic models for  $f=1$ Hz,  $q_{SAT}=1\mu C$ ,  $q_0=0.4\times q_{SAT}$ . (a) input and capacitor voltages, (b) memristor charge and memristance (c) memristor voltage and memristor current, (d) memristor zero-crossing hysteresis loops.  $v_C$  corresponds  $v_o$  for LP filter and  $v_{Mem}$  corresponds  $v_o$  for HP filter, respectively

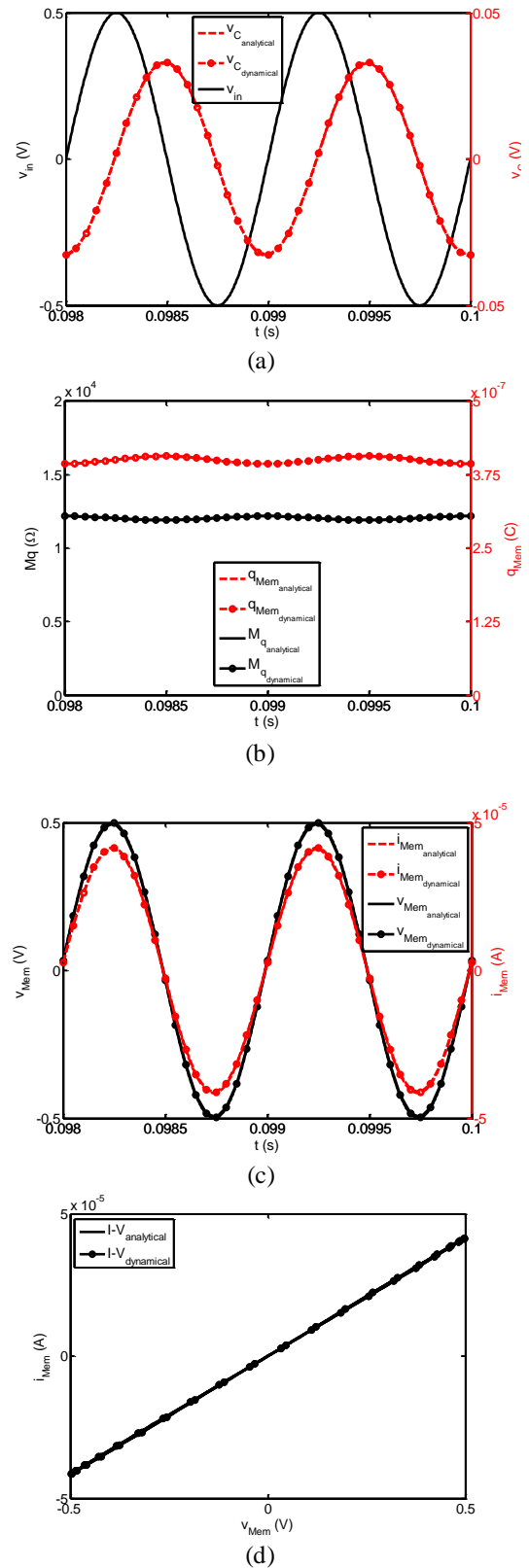


Fig. 3. M-C LP and HP filters time domain waveforms obtained using small signal and dynamic models for  $f=1$ kHz,  $q_{SAT}=1\mu C$ ,  $q_0=0.4\times q_{SAT}$ . (a) input and capacitor voltages, (b) memristor charge and memristance (c) memristor voltage and memristor current, (d) memristor zero-crossing hysteresis loops.  $v_C$  corresponds  $v_o$  for LP filter and  $v_{Mem}$  corresponds  $v_o$  for HP filter, respectively

### 5.2. Inspection of the gain of the memristor-based low-pass and high-pass filters

Using the formulas obtained in Section 4.2 and the dynamic model, gain responses of LP and HP filters are demonstrated in Fig. 4 and Fig. 5, respectively. The filter gains for both models match very well as shown in Fig. 4 and Fig. 5.

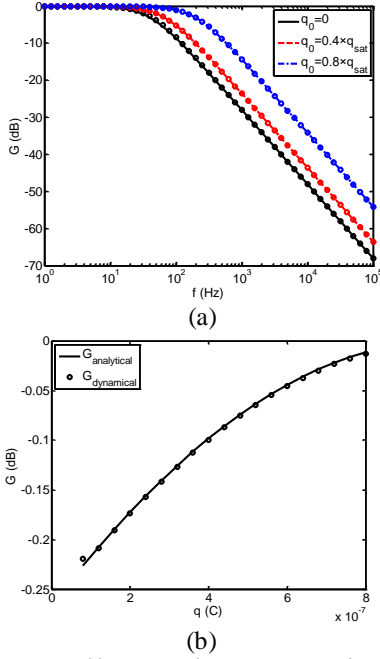


Fig. 4. M-C LP filter gain characteristics obtained using small signal and dynamic models for  $q_{SAT}=1\mu C$ , (a) with respect to frequency for three different initial charge ( $q_0$ ) values (b) with respect to initial charge for  $f=10Hz$ .

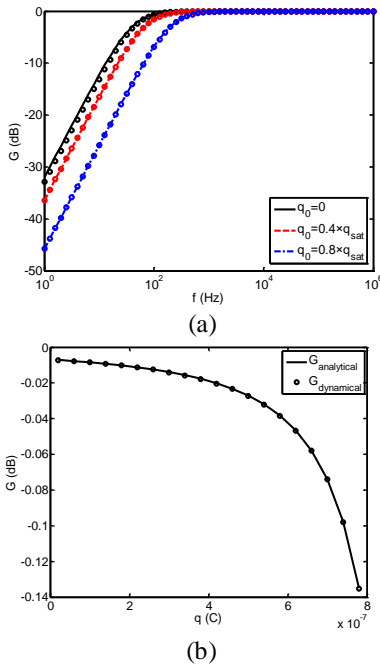


Fig. 5. M-C HP filter gain characteristics obtained using small signal and dynamic models for  $q_{SAT}=1\mu C$ , (a) with respect to frequency for three different initial charge ( $q_0$ ) values (b) with respect to initial charge ( $q_0$ ) for  $f=1kHz$ .

### 5.3. Inspection of the total harmonic distortion of the memristor-based low-pass and high-pass filters

Using the formulas obtained in Section 4.3 and the dynamic model, the total harmonic distortions of both LP and HP filters are demonstrated in Fig. 6 and Fig. 7, respectively. The THDs of the M-C LP and HP filters for both models match well as shown in Fig. 6 and Fig. 7.

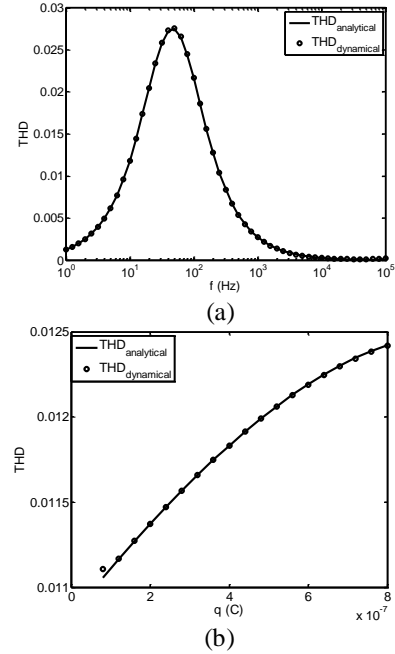


Fig. 6. M-C LP filter THD characteristics obtained using small signal and dynamic models for  $q_{SAT}=1\mu C$ , (a) with respect to frequency for  $q_0=0.4\times q_{SAT}$  (b) with respect to initial charge for  $f=10Hz$ .

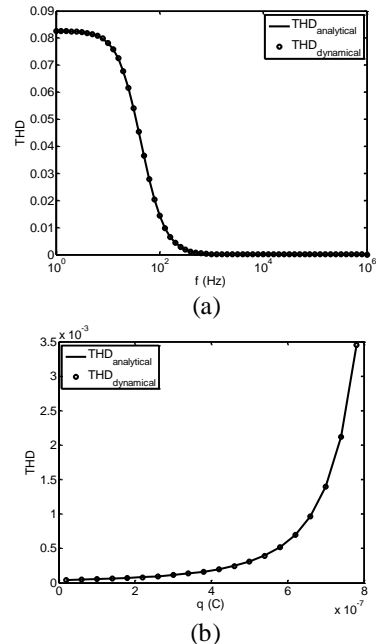


Fig. 7. M-C HP filter THD characteristics obtained using small signal and dynamic models for  $q_{SAT}=1\mu C$ , (a) with respect to frequency for  $q_{SAT}=1\mu C$ , (b) with respect to initial charge for  $f=1kHz$ .

## 6. Conclusions

Memristor is a nonlinear element and therefore, memristor-based circuits are also nonlinear. Due to this non-linearity, many memristor-based applications cannot be solved analytically. In this study, using perturbation method, small-signal models of both of the TiO<sub>2</sub> linear drift model memristor-based low-pass and high-pass filters are derived for the first time in literature. Their time-domain responses are obtained and the validity of the small-signal models are examined with simulations using dynamic models. Simulations have shown that the results of perturbation method for memristor based filters are in good agreement with that of the numerical simulations. The small signal models are able to predict circuit waveforms, hysteresis loop of the memristor, and also gains of the memristor-based LP and HP filters accurately as long as keeping  $\varepsilon$  a small number.

As a figure of merit, the total harmonic distortion (THD) of both type of filters for small signals are also given and the small signal models are also able to calculate THD of the filters very accurately. Using the small signal models, THD behavior of the memristor-based LP and HP filters are also examined in this study. It has been found that the THD of the memristor-based LP filter for small signals is zero at zero frequency, starts increasing with increasing frequency, becomes maximum at a frequency, which is equal to  $1/\sqrt{2}$  times the cut-off frequency, starts decreasing after the maximum point, and disappears at high frequencies. The THD of the memristor-based HP filter is maximum at zero frequency and is a monotonously decreasing function. Both THDs of the memristor-based LP and HP filters always tend to decrease and becomes negligible at high frequencies.

Memristor is a new nonlinear circuit element; its combinations with other circuit elements have not been completely understood yet. That's why the analysis of the filter circuits with (a) memristor(s) is very important and analysis of them can provide a better understanding of their behavior and new design guides so that, in the future, when memristor becomes available in market, its potential can be fully exploited and memristor-based filter circuits with a good-performance can be designed. Based on the experience gained in this paper, we also suggest that perturbation theory can be used to analyze other memristor-based filters or circuits with models other than linear drift model.

## References

- [1] L. O. Chua, *IEEE Trans. Circuit Theory* **18**(5), 507 (1971).
- [2] D. B. Strukov, et al., *Nature* **453**(7191), 80 (2008).
- [3] O. Kavehei, et al., *Proc. R. Soc. A Math. Phys. Eng. Sci.* **466**(2120), 2175 (2010).
- [4] R. Mutlu, *Turkish J. Electr. Eng. Comput. Sci.* **23**(5), 1219 (2015).
- [5] Y. V. Pershin, M. Di Ventra, *IEEE Trans. Circuits Syst. I Regul. Pap.* **57**(8), 1857 (2010).
- [6] S. Shin, et al., *IEEE Trans. Nanotechnol.* **10**(2), 266 (2011).
- [7] T. A. Wey, W. D. Jemison, *IET Circuits, Devices Syst.* **5**(1), 59 (2011).
- [8] Y. V. Pershin, et al., *J. Comput. Theor. Nanosci.* **8**(3), 441 (2011).
- [9] T.-W. Lee, J. H. Nickel, *IEEE Electron Device Lett.* **33**(10), 1456 (2012).
- [10] E. Kyriakides, J. Georgiou, *Int. J. Circuit Theory Appl.* **43**(11), 1801 (2015).
- [11] M. A. Zidan, et al., *Int. J. Circuit Theory Appl.* 2013, p. in press.
- [12] Ş. Ç. Yener, *New Opportunities in Analog Circuit Design Provided by Memristor*, İstanbul Technical University, Institute of Science and Technology, PhD Thesis, 2014.
- [13] Ş. Ç. Yener, H. H. Kuntman, *Radioengineering* **23**(4), 1140 (2014).
- [14] Ş. Ç. Yener, et al., *Analog Integr. Circuits Signal Process* **89**(3), 719 (2016).
- [15] M. E. Fouda, A. G. Radwan, *Int. J. Circuit Theory Appl.* **42**(10), 1092 (2014).
- [16] S. C. Yener, et al., 2017 Electric Electronics, Computer Science, Biomedical Engineerings' Meeting, EBBT 2017. IEEE, 2017, p. 1–3.
- [17] S. C. Yener, et al., *Acta Phys. Pol. A*, **132**(3–II), 1058 (2017).
- [18] A. Ascoli, et al., 14th Latin American Test Workshop (LATW2013). IEEE, 2013, p. 1–6.
- [19] Z. J. Chew, L. Li, *Electron. Lett.* **48**(25), 1610 (2012).
- [20] T. Driscoll, et al., *Appl. Phys. Lett.* **97**(9), 93502–1 (2010).
- [21] M. S. Qureshi, et al., *Electron. Lett.* **48**(13), 757 (2012).
- [22] W. Wang, et al., *International Conference on Communications, Circuits and Systems*, 969 (2009).
- [23] S. C. Yener, et al., *Optoelectron. Adv. Mat.* **9**(1–2), 266 (2015).
- [24] Ş. Ç. Yener, et al., *Inf. MIDEM - J. Microelectron. Electron. Components Mater.* **44**(2), 109 (2014).
- [25] K. E. Avrachenkov, *Analytic Perturbation Theory and Its Applications Analytic Perturbation Theory and Its Applications 2013*.
- [26] R. E. Bellman, *Perturbation techniques in mathematics, physics, and engineering*, New York: Dover Publications, 1972.
- [27] C. M. Bender, S. A. Orszag, *Advanced mathematical methods for scientists and engineers I: Asymptotic methods and perturbation theory*, New York: Springer, 1999.
- [28] F. M. Fernández, *Introduction to perturbation theory in quantum mechanics*, Florida: CRC press, 2010.